Estimates of Europa's ice shell thickness from elastically-supported topography

F. Nimmo[1]
Department of Earth Sciences, University College London, London, UK

B. Giese
Deutsches Zentrum für Luft- und Raumfahrt, Berlin, Germany

R. T. Pappalardo
Laboratory for Atmospheric and Space Physics, University of Colorado, Boulder, Colorado, USA

Received 24 November 2002; revised 6 January 2003; accepted 3 February 2003; published 11 March 2003.

[1] The thickness of Europa's solid ice shell is uncertain, and has important implications for Europa's habitability and thermal history, and the design of future spacecraft missions. Here we obtain an estimate of the ice shell thickness from observations of a plateau SW of Cilix impact crater. Stereo topographic profiles suggest that the plateau is flexurally supported, with an effective elastic thickness t_e of 6^{+5}_{-2} km. For a conductive temperature profile this t_e value implies a solid ice shell thickness of 15^{+20}_{-9} km; if the shell is convecting, this estimate is a lower bound. Combined with independent estimates, we infer a probable shell thickness of ≈25 km. The shell thickness is likely to be uniform over the entire satellite. *INDEX TERMS:* 6218 Planetology: Solar System Objects: Jovian satellites; 5418 Planetology: Solid Surface Planets: Heat flow; 5475 Planetology: Solid Surface Planets: Tectonics (8149); 8122 Tectonophysics: Dynamics, gravity and tectonics; 8160 Tectonophysics: Evolution of the Earth: Rheology—general. **Citation:** Nimmo, F., B. Giese, and R. T. Pappalardo, Estimates of Europa's ice shell thickness from elastically-supported topography, *Geophys. Res. Lett.*, *30*(5), 1233, doi:10.1029/2002GL016660, 2003.

[2] Jupiter's satellite Europa is believed to possess a ~100 km deep liquid water layer beneath its icy shell [*Pappalardo et al.*, 1999; *Kivelson et al.*, 2000], and is therefore a potential abode for life [*Chyba and Phillips*, 2001]. The thickness of the solid shell has important implications for the shell dynamics, nutrient transport [*Chyba and Phillips*, 2001], the thermal history of the satellite [*Pappalardo et al.*, 1998; *Greenberg et al.*, 2000; *Hussmann et al.*, 2002], and the design of future spacecraft missions [e.g., *Chyba et al.*, 1998]. However, the solid shell thickness is not well known: estimates vary from 1–2 km [*Hoppa et al.*, 1999a; *Greenberg et al.*, 2000] to a few tens of km [*Pappalardo et al.*, 1998; *Rathbun et al.*, 1998]. Recently, two impact crater studies have derived lower bounds of 3–4 km [*Turtle and Pierazzo*, 2001] and 19 km [*Schenk*, 2002], respectively. Here we use a model of topographic support on Europa to obtain an independent constraint on its shell thickness.

[3] Topography on the Earth and other bodies is supported by a variety of mechanisms [e.g., *Watts*, 2001]. Short wavelength loads are often flexurally supported by the rigidity of cold, near-surface material. Longer wavelength loads may be supported by lateral variations in crustal thickness or density (isostasy), or by dynamic processes such as convection. Similar processes are likely to maintain topography on the icy satellites of the outer solar system.

[4] The ability of a body to support a load through flexure may be described by its effective elastic thickness t_e [e.g., *Watts*, 2001]. Estimates of t_e based on topography have mostly produced rather small values for icy satellites: 0.15–2.6 km for Europa [*Tufts et al.*, 1997; *Williams and Greeley*, 1998; *Billings and Kattenhorn*, 2002], and 0.9–1.7 km for Ganymede [*Nimmo et al.*, 2002]. A study by *Figueredo et al.* [2002] of Murias Chaos, Europa, produced a larger value of $t_e \approx 4 \pm 2$ km, but these authors did not relate this value to the solid shell thickness.

[5] Here we focus on an area south-west of Cilix crater (3°N, 182°W), Europa. Figure 1 shows a Galileo image of the area, with Cilix in the northern portion. The area is relatively uncratered, consistent with a young surface age for Europa of about 50 My [*Zahnle et al.*, 1998], and is heavily deformed by several generations of double ridges, which generally trend in an easterly to north-easterly direction. At least some dark material in the area is associated with Cilix and may have been excavated by the impact. A region of disrupted material (a "lenticula") 12 km across in its shortest dimension is located 60 km to the SW of Cilix.

[6] Figure 1 also shows a digital elevation model (DEM) of the same area, derived by combining the 120 m/pixel image shown with six 70 m/pixel Galileo images to form stereo pairs [*Giese et al.*, 1999]. The horizontal resolution of the DEM is ~500 m and the vertical resolution 30–60 m. The central peak, surrounding basin and elevated rim of Cilix are clearly visible in the DEM, as are some of the more prominent double ridges. Of particular interest is a 30–40 km wide plateau-like feature in the west of the image, which is bounded on both the NW and SE sides by shallow topographic lows, and to the NE by a sharp fracture. The origin of the topography is unclear. It may be related to Cilix, about one crater diameter distant; alternatively, the lenticula to the SW may be evidence for diapirism.

[1]On leave at Department of Earth and Space Sciences, University of California, Los Angeles, California, USA.

0094-8276/03/2002GL016660$05.00

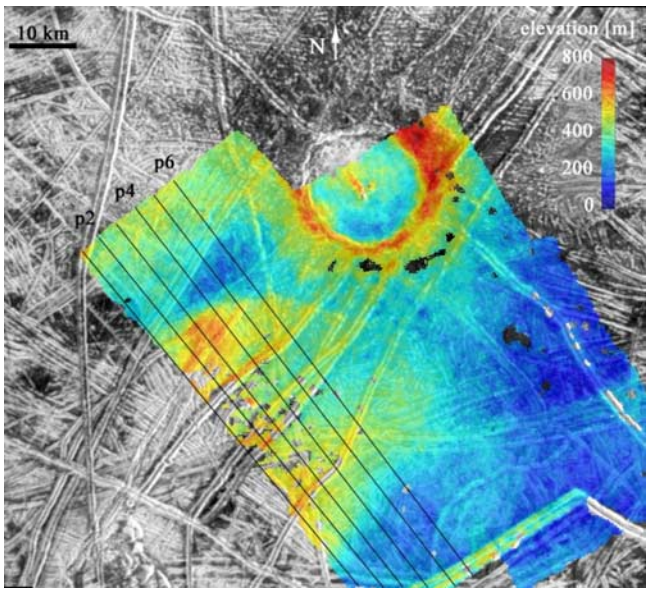

Figure 1. Galileo image of Cilix crater and surroundings with superimposed stereo-derived topography (color). Background image resolution 120 m/pixel. Topography horizontal resolution 500 m, vertical resolution 30–60 m.

[7] Figure 2 shows a series of topographic profiles across this plateau. It demonstrates relatively steep scarps (slope ≈ 2°) to the north and south, with a moat outboard of the scarps. The edges of the plateau are higher than the center. The plateau profile differs from the convex or flat-topped uplift expected from convective support [e.g., *Watts*, 2001]. If the plateau is high because of compositional buoyancy, it is hard to explain the flanking moats. Irrespective of the original mode of formation, we show below that both the moats and the depression at the center of the plateau are to be expected if the plateau is supported elastically today. While the plateau morphology could potentially be explained by more complex rheologies (e.g., viscoplastic [*Dombard and McKinnon*, 2001]), we adopt a simple elastic model in view of the large uncertainties in other parameters.

[8] A material's rigidity, D, is related to its effective elastic thickness t_e by [e.g., *Watts*, 2001]

$$D = \frac{E t_e^3}{12(1-\nu^2)}, \tag{1}$$

where E is the Young's modulus and ν is the Poisson's ratio. The deflection w of a plate under a sinusoidal topography of amplitude h and density ρ_c is given by

$$w = \frac{h\rho_c}{\rho_m - \rho_c + Dk^4/g} \tag{2}$$

where ρ_c is the density of the deflected material, ρ_m is the density of the underlying substrate, k is the wavenumber and g is the acceleration due to gravity. If the rigidity is zero, the deflection occurs such that the load is supported by shell thickness variations. If the base of the solid shell is not deflected, we set $\rho_m = \rho_c$.

[9] Any specified load may be represented by its Fourier components, and the deflection w associated with each component calculated using equation (2). The resulting topography can then be obtained by taking the inverse Fourier transform. Here we assume a trapezoidal load (see Figure 3), where the x-coordinates of the vertices are fixed. We vary t_e, the y-coordinates of the vertices (y_1, y_2), and a DC offset to the model topography to minimize the RMS misfit of the model to the observations.

[10] Figure 3a shows the mean topography of profiles p1–p6, obtained by stacking them using the northern plateau scarp as a fixed point. The dashed lines show the standard deviation about the mean. The bold line is the best-fit model flexural profile, calculated using the method described above and model parameters given in the figure caption. The best-fit elastic thickness is 6.0 km. The fit to the topography is generally within one standard deviation, except at the far southern end of the profile.

[11] Figure 3b shows the local minimum value of the RMS misfit H as a function of t_e (solid line). The existence of a minimum misfit, H_{min} is obvious for the stacked profile; it is also clear that H increases rapidly for values of t_e less than the best-fit value. For a misfit range of $1.2H_{min}$, the acceptable range of t_e is 4.6–9.4 km. The dotted lines in Figure 3b are misfit plots of the fit to the individual profiles p1, p3 and p5 of Figure 2. They all show that small values of t_e produce unacceptably high misfits, and have best fit t_e values in the range 4.9–11.9 km.

[12] Since the northern flexural moat is more obvious, and t_e may also vary along trend, we also perform a fit using only the northern half of the stacked profile. Doing so results in a halving of the misfit, but an almost identical elastic thickness (t_e = 5.5 km). We assume that the $\rho_c = \rho_m$, for reasons discussed below; if the shell thickness does vary laterally, the best fit to the entire profile has a t_e of 5.7 km. We also assume an unbroken elastic plate. Broken plates deflect more for a given load [e.g., *Watts*, 2001]; thus, if the plate is in fact broken, our elastic thickness estimates are again conservatively low. Similarly, while we are using a Cartesian geometry, adopting an axisymmetric geometry typically produces slightly higher t_e values [*Figueredo et al.*, 2002].

[13] The correct value of E for ice is uncertain; values derived from small homogeneous laboratory samples are typically larger than those derived from terrestrial field

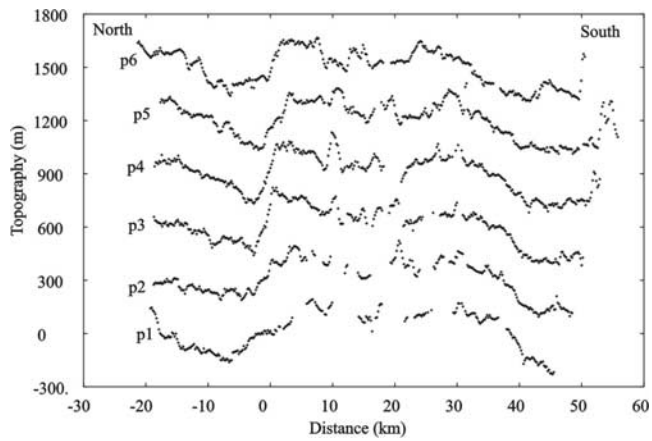

Figure 2. Topographic profiles p1–p6 (locations in Figure 1). A vertical offset of 300 m was added to each successive profile. Profiles are aligned on the N plateau scarp to enable stacking (see Figure 3).

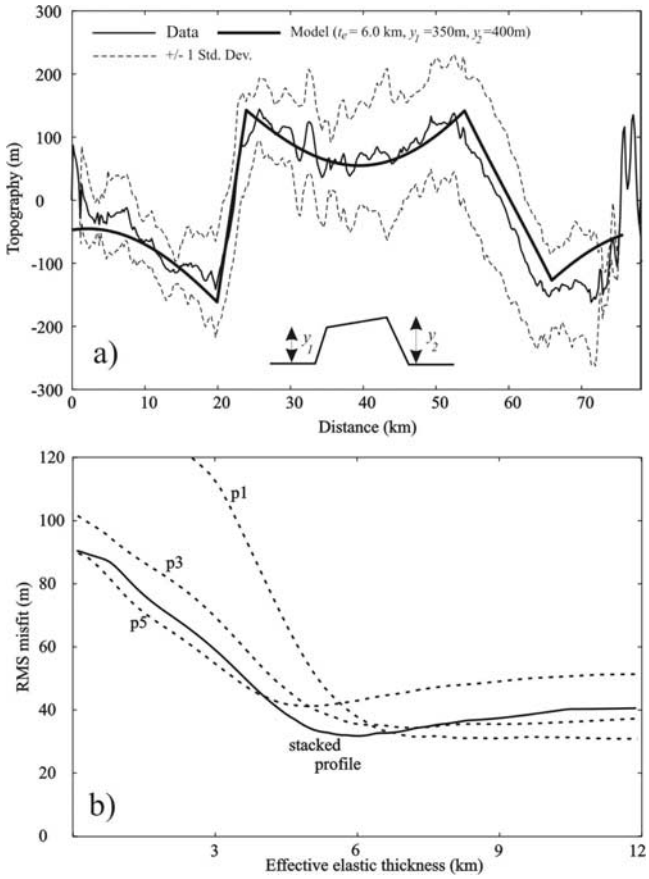

Figure 3. (a) Stacked topographic profile, after removal of mean and a linear trend joining the end-points. Raw data were linearly interpolated to 0.2 km spacing and a linear trend joining the end points was removed prior to stacking. Solid line is the mean; dashed lines are ± one standard deviation (std. dev.) plotted where the number of profiles exceeds 2. Bold line is best-fit flexural profile assuming an initially trapezoidal load geometry (see inset) with an elastic thickness t_e of 6.0 km, y_1 = 350 m, y_2 = 400 m. The zone of computation for the theoretical profile extends 20 km beyond each end of the figure. The constants assumed were: g = 1.3 m s^{-2}, $\rho_m = \rho_c$ = 900 kg m^{-3}, E = 1 GPa, ν = 0.3. (b) Minimum RMS misfit as a function of t_e. Solid line is misfit function for profile in a); dashed lines are misfit functions for individual profiles as labeled.

studies [*Vaughan*, 1995; *Budd and Jacka*, 1989]. We use here a value of 1 GPa from terrestrial modelling of tidally-flexed ice sheets [*Vaughan*, 1995]. Laboratory studies give a value of 9 GPa [*Petrenko and Whitworth*, 1999], which by equation (1) would imply t_e = 2.9 km for the best-fit profile. We consider that the field studies are more likely to reproduce conditions on Europa than the laboratory samples, and thus adopt the lower value for E.

[14] The depth to which ice can maintain long-term elastic strength depends on both temperature and strain rate. At low strain rates or high temperatures, the ice will deform in a ductile fashion and the elastic stresses will be relaxed. For a given strain rate, there is thus a characteristic temperature T_R which defines the base of the elastic layer [*Nimmo et al.*, 2002]. Since the increase in temperature with depth depends on the thickness of the entire ice crust, the elastic thickness may be used to infer the crustal thickness. For the conducting part of the ice shell, in which conductivity varies as $1/T$ [*Klinger*, 1980], we have

$$\frac{t_c}{t_e} = \frac{\ln(T_B/T_S)}{\ln(T_R/T_S)} \tag{3}$$

where T_S is the surface temperature (105 K [*McKinnon*, 1999]), t_c is the thickness of the conducting layer and T_B is the temperature at the base of this layer. If the ice is not convecting, t_c is the total shell thickness and T_B is the melting temperature (260–270 K). If the ice is convecting, t_c is the conducting (stagnant) lid thickness and T_B is the temperature of the convective interior (250–260 K [*McKinnon*, 1999; *Nimmo and Manga*, 2002]).

[15] On Earth, the homologous temperature (the ratio of the temperature of interest to the melting temperature) at the base of the elastic layer is 0.6 ± 0.05 [e.g., *Watts and Daly*, 1981]. A wide range of materials show changes in material properties at similar homologous temperatures [e.g., *Frost and Ashby*, 1982]. If applicable to Europa, this ratio would imply T_R = 159 ± 17 K. *Nimmo et al.* [2002] used viscoelastic calculations and realistic ice rheologies to calculate T_R as a function of (constant) strain rate. These calculations are appropriate as long as the stresses caused by emplacement of the load exceed the tidal stresses; it will be shown below that this criterion is satisfied. For a likely upper bound on strain rate of the present-day value of 2×10^{-10} s^{-1} [*Ojakangas and Stevenson*, 1989] *Nimmo et al.* [2002] found that $T_R \leq 185$ *K*. Although lower strain rates give lower values of T_R, the upper bound on strain rate is more important, since this will place a lower bound on the shell thickness (equation 3). The period of Europa's non-synchronous rotation is $\geq 10^4 a$ [*Hoppa et al.*, 1999b], implying strain rates $\leq 10^{-14}$ s^{-1}. If non-synchronous rotation is the dominant cause of deformation, $T_R \leq$ 140 K. Equation (3) therefore implies that the ratio of shell to elastic thicknesss t_c/t_e is greater than 1.5; for a likely value of T_R = 150 K and T_B = 260 K, the ratio is 2.5.

[16] With t_e and the ratio t_c/t_e both known, the thickness of the conducting part of the ice shell may be calculated directly. The most likely value is 15 km (2.5 × 6 km); for minimum values of t_e = 4 km and t_c/t_e = 1.5, t_c is 6 km. In fact, this value is likely to be an underestimate, since the top kilometer or so of ice will be heavily fractured and lack significant elastic strength. For likely bounds of T_R = 140 K and t_e = 11 km, the upper limit on t_c is 35 km. Note also that if the ice is convecting, t_c will underestimate the total shell thickness.

[17] An important feature of flexural profiles is that they record the lowest value of t_e since the load was emplaced [e.g., *Watts*, 2001]. The value of t_e derived above is therefore a minimum estimate of the present-day t_e, and hence a minimum estimate of the shell thickness. Values of t_e smaller than that derived here [*Tufts et al.*, 1997; *Williams and Greeley*, 1998; *Billings and Kattenhorn*, 2002] are probably records of an earlier time or specific location where the conducting lid thickness was smaller, and may not record the present-day value of t_e at those locations.

[18] The elastic thickness estimate obtained is local to one area of Europa, and may thus not be representative. However, it is clear that, in at least this one area, the shell has been relatively thick since the load was emplaced. The

low viscosity of ice close to its melting temperature ensures that lateral shell thickness variations will be removed on timescales of 10^2–10^5 years [*Stevenson*, 2000], unless the ice shell is $\leq$6 km thick [*O'Brien et al.*, 2002]. This rapid lateral flow is the reason for assuming that the base of the shell is flat, and means that the topography cannot be supported by Airy isostasy. It also strongly implies that Europa's present-day shell thickness is uniform everywhere [*Stevenson*, 2000]. As noted above, smaller values of t_e derived elsewhere on Europa do not necessarily imply locally smaller values in present-day shell thickness.

[19] Treating the ice shell of Europa as an elastic shell overlying an inviscid medium is undoubtedly a simplification of the real problem. While the analysis of *Nimmo et al.* [2002] incorporates the dependence of effective t_e on strain rate, it does not address the effects of stress-dependent viscosity or variable strain rate on viscoelastic relaxation. Although these effects could be incorporated, in the absence of observations of how deformation on Europa has varied as a function of time or loading age, it is not clear that more complex models are justified. Similarly, many terrestrial workers still use purely elastic models [e.g., *McKenzie and Fairhead*, 1997].

[20] Given a conducting layer thickness, other parameters of interest to the thermal history of Europa may be calculated. For T_R = 150 K and t_e = 6 km, the local heat flux is 34 mW m^{-2}, somewhat larger than the global upper limit of 25 mW m^{-2} estimated by *Hussmann et al.* [2002]. The stresses present in the elastic layer of Figure 3 are a few MPa. While these stresses are 1–2 orders of magnitude larger than present-day tidal stresses [*Greenberg et al.*, 1998; *Moore and Schubert*, 2000], they are similar to the stresses which would be expected if Europa is rotating in a non-synchronous fashion or underwent polar wander [*Leith and McKinnon*, 1996]. Futhermore, the frictional stress at the base of a 1–2 km thick brittle layer will also be $\sim$1 MPa [*Golombek and Banerdt*, 1990]. There is thus a broad agreement between the stresses required to cause brittle or elastic deformation, and the likely driving stresses available.

[21] There are now three independent estimates of Europa's shell thickness which are mutually self-consistent: impact crater constraints ($t_c \geq$ 19 km [*Schenk*, 2002]); convective tidal dissipation models ($t_c \approx$ 25–50 km [*Hussmann et al.*, 2002]); and the flexural results presented here ($t_c = 15^{+20}_{-9}$ km). These combined results together suggest a uniform present-day shell thickness for Europa close to 25 km.

[22] **Acknowledgments.** This work was supported by NASA PGG and the Royal Society. We thank Patricio Figueredo and an anonymous reviewer, whose comments greatly improved this manuscript.

References

Billings, S. E., and S. A. Kattenhorn, Determination of ice crust thickness from flanking cracks along ridges on Europa (abstract), *Lunar Planet. Sci.*, *XXXIII*, 1813, 2002.

Budd, W. F., and T. H. Jacka, A review of ice rheology for ice-sheet modeling, *Cold Reg. Sci. Technol.*, *16*, 107–144, 1989.

Chyba, C. F., and C. B. Phillips, Possible ecosystems and the search for life on Europa, *Proc. Natl. Acad. Sci.*, *98*, 801–804, 2001.

Chyba, C. F., S. J. Ostro, and B. C. Edwards, Radar detectability of a subsurface ocean on Europa, *Icarus*, *134*, 292–302, 1998.

Dombard, A. J., and W. B. McKinnon, Formation of grooved terrain on Ganymede: Extensional instability mediated by cold, superplastic creep, *Icarus*, *154*, 321–336, 2001.

Figueredo, P., F. C. Chuang, J. Rathbun, R. L. Kirk, and R. Greeley, Geology and origin of Europa's "Mitten" feature (Murias Chaos), *J. Geophys. Res.*, *107*(E5), 5026, 10.1029/2001JE001591, 2002.

Frost, H. J., and M. F. Ashby, *Deformation-Mechanism Maps: The Plasticity and Creep of Metals and Ceramics*, Pergamon, New York, 1982.

Giese, B., R. Wagner, G. Neukum, and J. M. Moore, The local topography of Europa's crater Cilix derived from Galileo SSI stereo images (abstract), *Lunar Planet. Sci.*, *XXX*, 1709, 1999.

Golombek, M. P., and W. B. Banerdt, Constraints on the subsurface structure of Europa, *Icarus*, *83*, 441–452, 1990.

Greenberg, R., et al., Tectonic processes on Europa: Tidal stresses, mechanical response, and visible features, *Icarus*, *135*, 64–78, 1998.

Greenberg, R., P. Geissler, B. R. Tufts, and G. V. Hoppa, Habitability of Europa's crust: The role of tidal-tectonic processes, *J. Geophys. Res.*, *105*, 17,551–17,562, 2000.

Hoppa, G. V., B. R. Tufts, R. Greenberg, and P. E. Geissler, Formation of cycloidal features on Europa, *Science*, *285*, 1899–1902, 1999a.

Hoppa, G. V., et al., Rotation of Europa: Constraints from terminator and limb positions, *Icarus*, *137*, 341–347, 1999b.

Hussmann, H., T. Spohn, and K. Wieczerkowski, Thermal equilibrium states of Europa's ice shell: Implications for internal ocean thickness and surface heat flow, *Icarus*, *156*, 143–151, 2002.

Kivelson, M. G., et al., Galileo magnetometer measurements: A stronger case for a subsurface ocean at Europa, *Science*, *289*, 1340–1343, 2000.

Klinger, J., Influence of a phase transition of ice on the heat and mass balance of comets, *Science*, *209*, 271–272, 1980.

Leith, A. C., and W. B. McKinnon, Is there evidence for polar wander on Europa?, *Icarus*, *120*, 387–398, 1996.

McKenzie, D., and D. Fairhead, Estimates of the effective elastic thickness of the continental lithosphere from Bouguer and free air gravity anomalies, *J. Geophys. Res.*, *102*, 27,523–27,552, 1997.

McKinnon, W. B., Convective instability in Europa's floating ice shell, *Geophys. Res. Lett.*, *26*, 951–954, 1999.

Moore, W. B., and G. Schubert, The tidal response of Europa, *Icarus*, *147*, 317–319, 2000.

Nimmo, F., and M. Manga, Causes, characteristics and consequences of convective diapirism on Europa, *Geophys. Res. Lett.*, *29*(23), 2109, 10.1029/2002GL015754, 2002.

Nimmo, F., R. T. Pappalardo, and B. Giese, Effective elastic thickness and heat flux estimates on Ganymede, *Geophys. Res. Lett.*, *29*(7), 1158, 10.1029/2001GL013976, 2002.

O'Brien, D. P., P. Geissler, and R. Greenberg, A melt-through model for chaos formation on Europa, *Icarus*, *156*, 152–161, 2002.

Ojakangas, G. W., and D. J. Stevenson, Thermal state of an ice shell on Europa, *Icarus*, *81*, 220–241, 1989.

Pappalardo, R. T., et al., Geological evidence for solid-state convection in Europa's ice shell, *Nature*, *391*, 365–368, 1998.

Pappalardo, R. T., et al., Does Europa have a subsurface ocean? Evaluation of the geological evidence, *J. Geophys. Res.*, *104*, 24,015–24,055, 1999.

Petrenko, V. F., and R. W. Whitworth, *Physics of Ice*, Oxford Univ. Press, New York, 1999.

Rathbun, J. A., G. S. Musser, and S. W. Squyres, Ice diapirs on Europa: Implications for liquid water, *Geophys. Res. Lett.*, *25*, 4157–4160, 1998.

Schenk, P. M., Thickness constraints on the icy shells of the Galilean satellites from a comparison of crater shapes, *Nature*, *417*, 41–421, 2002.

Stevenson, D. J., Limits on the variation of thickness of Europa's ice shell (abstract), *Lunar Planet. Sci.*, *XXXI*, 1506, 2000.

Tufts, R., R. Greenberg, P. Geissler, G. Hoppa, R. Pappalardo, and R. Sullivan, Crustal displacement features on Europa, *Geol. Soc. Am. Abstr. Programs*, *29*, A-312, 1997.

Turtle, E. P., and E. Pierazzo, Thickness of a Europan ice shell from impact crater simulations, *Science*, *294*, 1326–1328, 2001.

Vaughan, D. G., Tidal flexure at ice shelf margins, *J. Geophys. Res.*, *100*, 6213–6224, 1995.

Watts, A. B., *Isostasy and Flexure of the Lithosphere*, Cambridge Univ. Press, New York, 2001.

Watts, A. B., and S. F. Daly, Long wavelength gravity and topography anomalies, *Annu. Rev. Earth Planet. Sci.*, *9*, 415–448, 1981.

Williams, K. K., and R. Greeley, Estimates of ice thickness in the Conamara Chaos region of Europa, *Geophys. Res. Lett.*, *25*, 4273–4276, 1998.

Zahnle, K., L. Dones, and H. F. Levison, Cratering rates on the Galilean satellites, *Icarus*, *136*, 202–222, 1998.

B. Giese, DLR, Rutherfordstrasse 2, 12489 Berlin, Germany. (bernd.giese@dlr.de)

F. Nimmo, Department of Earth Sciences, University College London, Gower St., London WC1E 6BT, UK. (nimmo@ess.ucla.edu)

R. T. Pappalardo, Laboratory for Atmospheric and Space Physics, University of Colorado, Campus Box 392, Boulder, CO 80309, USA. (robert.pappalardo@colorado.edu)